European Journal of Soil Science

European Journal of Soil Science, 2011 doi: 10.1111/j.1365-2389.2011.01381.x

Mapping soil clay contents in Dutch marine districts using gamma-ray spectrometry

E. van der Klooster[a], F. M. van Egmond[b] & M. P. W. Sonneveld[a]

[a]*Land Dynamics Group, Wageningen University, PO Box 47, 6700 AA Wageningen, the Netherlands, and* [b]*The Soil Company, Leonard Springerlaan 9, 9727 KB Groningen, the Netherlands*

Summary

Conventional soil sampling methods to obtain high-resolution soil data are labour intensive and costly. Recently, gamma ray spectrometry has emerged as a promising technique to overcome these obstacles. The objective of our study was to investigate the prediction of soil clay contents using gamma-ray spectrometry in three marine clay districts in the Netherlands: the southwestern marine district (SMD), the IJsselmeerpolder district (IJPD) and the northern marine district (NMD). The performance of linear regression models was investigated at field (<1 km^2), regional ($1-1000$ km^2) and district (>1000 km^2) scales and for all the Dutch marine districts together. For this study, a database was available with 1371 gamma-ray spectra measured on arable fields in marine clay districts during the period 2005–2008 and these were all linked to laboratory analyses of clay contents. At the field scale, linear regression models based on ^{40}K, ^{232}Th, or a combination of these revealed much smaller root mean squared error (RMSE) values (2–3%) compared with a model based on the field mean (8–10%). At the district scale, the regression models for the SMD and IJPD, which have comparable sediments, performed better than for the NMD. This indicates that the prediction of clay contents in late Holocene marine sediments may be made with gamma-ray spectrometry provided that the origin of the parent material results in a unique fingerprint. Because of the heterogeneous parent material of all marine districts taken together, our study shows that no unique and precise fingerprint exists, and the RMSE of 6% between clay contents and gamma-ray spectra is not much different from the RMSE of 7% when using the overall mean as a predictor.

Introduction

Information on the spatial variability of soil properties is valuable for farmers, because spatial variability affects both yields and nutrient-use efficiencies. High-resolution spatial soil data may therefore increase the efficiency of inputs, especially in precision farming (Viscarra Rossel & McBratney, 1998; Van Alphen & Stoorvogel, 2000). Landscape reconstruction and environmental studies may also benefit from high-resolution spatial soil data (Kemmers *et al.*, 2008). However, conventional soil sampling methods for mapping soil properties at intensive spatial resolutions are costly. Gamma-ray spectrometry is one way of achieving a more cost-effective procurement of high-resolution soil data.

Rock and soils contain gamma radiation emitting radioactive isotopes, the most important of which are potassium-40 (^{40}K), thorium-232 (^{232}Th) and uranium-238 (^{238}U) and, in some parts of the world, ^{137}Cs. Although ^{40}K , ^{232}Th and ^{238}U are naturally occurring radio-nuclides, the occurrence of ^{137}Cs in Europe is primarily the result of the nuclear accident of Chernobyl in 1986, which had a fall-out pattern similar to the irregular rainfall patterns at that time (Frissel *et al.*, 1987; Köster *et al.*, 1987). The specific combination of the isotopes ^{40}K, ^{232}Th, ^{238}U and ^{137}Cs is characteristic of soil parent material and is associated with some soil properties. These relationships have been studied in two ways. One method, often used in mineralogy, is fingerprinting (De Meijer & Donoghue, 1995; Van Wijngaarden *et al.*, 2002; Hebinck *et al.*, 2007). Fingerprinting is based on the principle that sand and clay each have their own specific radiometric signal or range of ^{40}K and ^{232}Th concentrations. Soils of similar age that originate from the same parent material tend to have the same gamma-ray profile, called a fingerprint. In this way sediments from different lithological sources can be identified. For example, Cook *et al.* (1996) used gamma-ray spectrometry to distinguish between different parent materials in an area with strongly weathered soils in Western Australia.

The second approach investigates the relationship between gamma-ray and soil properties using various statistical methods. Rawlins *et al.* (2007) found good correlations between gamma-ray spectra of ^{40}K and ^{232}Th measured from the air and texture

Correspondence: M. P. W. Sonneveld. E-mail: marthijn.sonneveld@wur.nl

Received 2 April 2010; revised version accepted 10 May 2011

for young Holocene soils in England. For a limited number of samples from Dutch soils, Köster *et al*. (1988) found that radionuclide contents were significantly related to clay contents, but not to soil organic matter. For a study area in Australia, Wong & Harper (1999) found a good relationship between plant-available K and radiation from ^{40}K. These authors also found relationships between ^{40}K and clay, pH, total iron, total-phosphorus and organic carbon. Pracilio *et al*. (2006) reported good relationships between the radiometric signal and clay and plant-available K for weathered soils using gamma-ray measurements made from the air and regression trees. In the weathered Baltic shield of Scandinavia, cadmium levels were correlated with ^{238}U (Söderström & Eriksson, 2008). Viscarra Rossel *et al*. (2007) showed robust predictions with bagging-partial least squares regression (PLSR) for clay, coarse sand and Fe contents in the topsoil (0–15 cm) with hyperspectral gamma-ray energy spectra obtained with ground-based measurements.

Because gamma-ray emissions are not uniquely coupled with any soil property, their strength and spectral composition alone will not predict soil properties globally. However, within specific geomorphic units and regions with uniform lithology and geochemistry, valuable soil information may be extracted by using gamma radiation (De Meijer & Donoghue, 1995; Rawlins *et al*., 2007). So far, many gamma-ray spectrometry studies have been performed in relatively old weathered landscapes. Fewer studies have investigated its performance for mapping soil properties in young Holocene deltaic environments such as those found in the Netherlands (De Meijer & Donoghue, 1995; Van Egmond *et al*., 2010). The objective of the present study was to investigate the prediction of soil clay contents using gamma-ray spectrometry in marine clay districts in the Netherlands at different spatial scales. The performance of linear regression models was investigated at field (<1 km^2), regional (1–1000 km^2) and district (>1000 km^2) scales and for the Dutch marine clay area as a whole. The study was limited to arable fields, as this is the dominant land use in Dutch marine clay districts.

Materials and methods

Gamma-ray measurements

The data used in this study were collected with a proximal gamma spectrometer referred to as 'The Mole' (Van Egmond *et al*., 2010). The Mole is a gamma-ray spectrometer with a CsI-crystal of 70 × 150 mm. Spectral information is stored in 512 energy bands between 0.40 and 2.85 MeV. The Mole is mounted on a tractor at 30 cm above the ground surface and measures the gamma-ray signal that originates from the top 30 cm of the soil. The field of view for 95% of the radiation received is a radius of 3 m around the sensor. The shape and intensity of the spectra are not affected by measurement height (Hendriks, 2002). Soil moisture does affect the signal intensity: an increase of 10% in soil moisture results in a 10% decrease in intensity (De Groot *et al*., 2009), but this has no effect on the spectral balance. The soil moisture differences during measurement are not expected to be more than 10%. The clarity and pattern of the spatial distribution of ^{232}Th measured on adjacent arable fields (Figure 1) are only in part

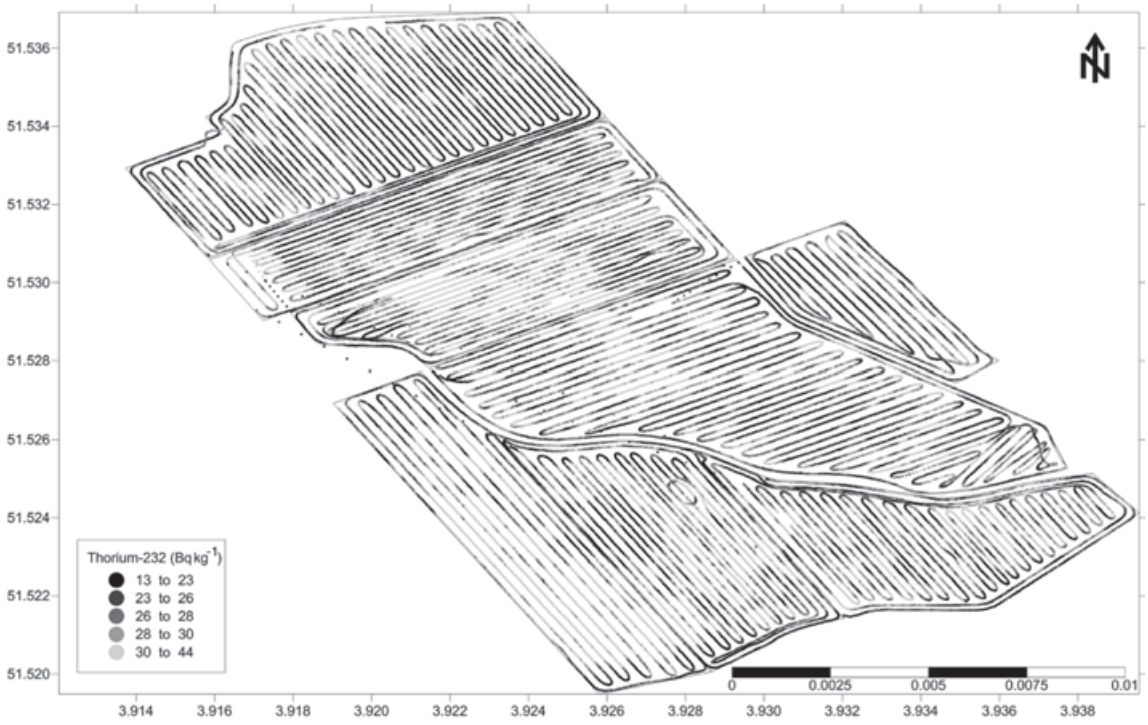

Figure 1 The spatial distribution of ^{232}Th on adjacent arable fields, measured during 2004.

attributed to differences in moisture content, and mainly to textural differences.

The database for this study contains 1371 gamma-ray spectra measured on arable fields in Dutch marine-clay districts during the period 2005–2008. These data are all linked to laboratory determinations of clay content.

Soil analyses

The data used in this study were not collected specifically for scientific purposes, but at farmers' requests in order to obtain high-resolution spatial soil information regarding their fields. Gamma radiation was measured on survey paths that together form a dense pattern (Figure 1). When fields were mapped for gamma radiation, soil samples were taken for laboratory analysis to calibrate the relationships between the measured gamma radiation and measured soil properties. These are the sample data that are used in this study. Soil sample locations were chosen on the basis of the variation in measured radiation per field by the total (energy) count (TC) displayed on a laptop computer. The locations of the samples were chosen to optimize coverage of the range in radiometric signals. During sampling, the spectrum was recorded for 300 s without moving the sensor. Soil samples were taken manually with a Dutch auger: at each sample location, six soil samples were taken from the top 30 cm randomly within the field of view of the sensor and were bulked to form one composite sample.

Clay contents were determined in the laboratory by either the pipette method or near-infrared spectroscopy (NIRS). The pipette method has a reported laboratory reproducibility (defined as $2\sqrt{2} \times$ standard deviation) of 2.5% for samples with <20% of clay content and 3.7% for samples with >20% of clay content. Near-infrared spectroscopy has a reported laboratory reproducibility of 5.6%.

Spectrum analysis

A commonly used index for gamma spectra is total count (TC), which sums the counts per energy channel over all energy channels. The main contributor to TC in this study was the concentration of ^{40}K (Hebinck *et al*., 2007). The full spectrum analysis method (FSA) was used to extract more specific information on the different radionuclides. With this method, the standard spectra of ^{40}K, ^{238}U, ^{232}Th and ^{137}Cs, with an activity of 1 Bq kg^{-1}, are fitted to the measured spectrum with a χ^2 algorithm. Multipliers of the standard spectra of the radionuclides are thus generated, which are equal to the activities of the different radio nuclides in Bq kg^{-1}. The uncertainty in the FSA method is at least a factor 1.7 less than in the more traditional windows method (Hendriks *et al*., 2001). Data with a fitted χ^2 value of >2 were omitted.

Study area

The study area is the marine area in the Netherlands, which is dominated by late Holocene sediments. This area is subdivided into three districts (Figure 2): the southwestern marine district (SMD), the northern marine district (NMD) and the IJsselmeerpolder district (IJPD) (De Bakker, 1979). The spatial stratification of Statistics Netherlands (1993) was used to delineate the districts.

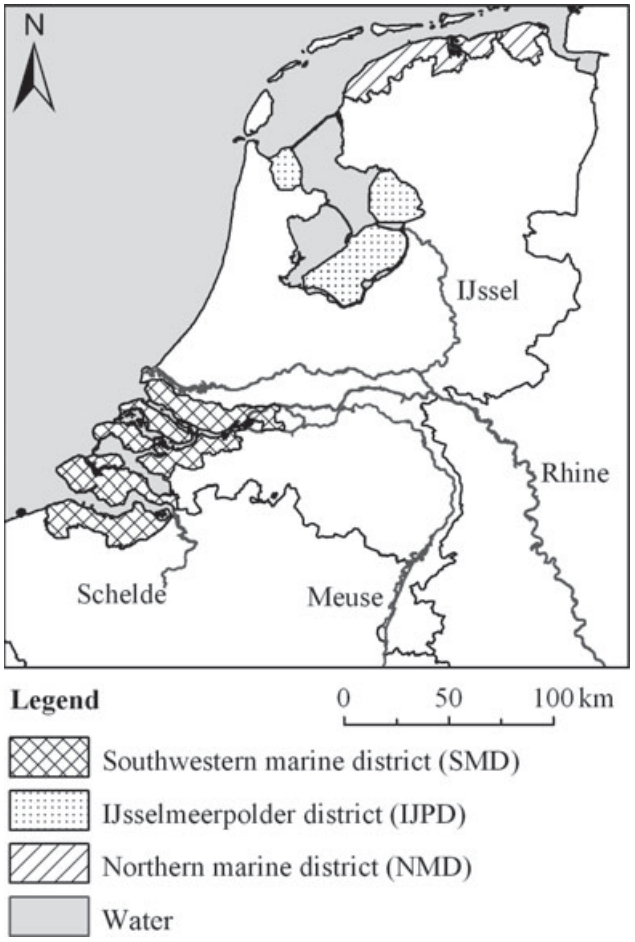

Figure 2 Overview of the selected marine districts and major rivers in the Netherlands.

The southwestern marine district covers approximately 3000 km^2. In the southwest, peaty forelands were covered with marine deposits between 1500 BC and 1200 AD. Former creeks in these forelands were filled with loamy deposits and clayey sediments were deposited on the surrounding peaty basin areas, which were later subjected to subsidence. The soils on the creek-ridges are mostly of the Dutch *Mn..A* soil series (De Bakker, 1979; Steur & Heijink, 1991), and are calcareous marine soils from tidal deposits with a physically ripened subsoil. Following the WRB classification (IUSS, 2006), these soils are classified as Calcaric Fluvisols. The surrounding lower-lying areas are classified as non-calcareous marine soils from tidal deposits with a physically unripened subsoil or peaty subsoil and are classified as the *Mn..C* Dutch soil series, which are (Histic) Fluvisols (IUSS, 2006). After 1200 AD, salt marshes were reclaimed from the sea. In these 'new-land' polders, the calcareous soils dominantly belong to the *Mn..A* soil series (De Bakker, 1979).

The IJsselmeerpolder district covers approximately 1100 km^2 and was reclaimed from the sea after the closure of the former Zuiderzee in 1932. Four polders have been cultivated since 1930, 1942, 1957 and 1968 (from north to south). The soils belong mainly to the calcareous *Mn..A* soil series.

The northern marine district covers approximately 1200 km^2 and was formed behind the coastal barrier islands of the Wadden Sea. On salt marsh barriers in this district, soils belong mainly to the calcareous *Mn..A* soil series and have relatively small clay contents, whereas in the salt marsh basins the soils mainly belong to the non-calcareous *Mn..C* soil series (De Bakker, 1979) or Haplic Fluvisols (IUSS, 2006) and have relatively larger clay contents. In some parts away from the coast, topsoils have swelling and shrinking properties with small Ca:Mg ratios and are non-calcareous. These belong to the *gMn..C* soil series (Stiboka, 1981; Steur & Heijink, 1991) or (Magnesic) Vertisols/Fluvisols (IUSS, 2006).

Sediments in the north and in the southwest of the Netherlands have different radiometric fingerprints (De Meijer & Donoghue, 1995). The SMD has been affected more by the Rhine, whereas the NMD has been affected more by sediments from the Elbe. In the IJPD, the influence of the Rhine has also been important, because the IJssel, a distributary of the Rhine, has deposited sediments here. However, before the closure of the Zuiderzee this area also received sediments from the Wadden Sea.

The digitized Dutch soil map at a scale 1:50 000 (De Vries *et al*., 2003) and the digital geomorphological map at scales 1:20 000–1:50 000 (Koomen & Maas, 2004) were used to delineate uniform areas with respect to major soil series and geomorphology. This resulted in a subdivision of districts into regions (Table 1). Note that the fields and districts are delineated by cadastral and administrative boundaries whereas the intermediate scale regions are delineated by physiographic boundaries.

Linear regression and model comparison

Relationships between laboratory-analysed clay content and the gamma radiation emitted were analysed at four spatial scales: field (<1 km^2), regional (1–1000 km^2), district (>1000 km^2) and the marine clay area as a whole. Linear regression models were derived to quantify the strength of the relationships using a generic expression. These were formulated with the general assumptions that accompany linear regression that, on average, the random error component is zero, the variance of the error component is constant, the separate values for the error component are uncorrelated and the error components are normally distributed. The general expressions were:

$$Clay\% = \beta_0 + (\beta_K \times {}^{40}\mathrm{K}) + (\beta_{\mathrm{Th}} \times {}^{232}\mathrm{Th}), \quad (1)$$

and

$$Clay\% = \beta_0 + \beta_{TC} \times \mathrm{TC}, \quad (2)$$

where *Clay%* is the clay content in % by mass, β_n are possible linear parameters, and ^{40}K, ^{232}Th (Bq kg^{-1}) and TC (digital count in s^{-1}) are possible explanatory variables. As gamma-ray emissions from all radionuclides contribute to TC, this characteristic is not independent of the individual radionuclides and is tested in a separate function. Emissions of the radionuclides ^{238}U and ^{137}Cs were omitted from our analyses because preliminary investigations did not show relationships with clay content, confirming the findings of Köster *et al*. (1988). In fingerprinting research, ^{40}K and ^{232}Th have also been shown to be the most important explanatory factors for the clay and sand content (De Meijer & Donoghue, 1995; Hebinck *et al*., 2007; Van Egmond *et al*., 2010).

The ^{40}K and ^{232}Th or TC data were used only as explanatory variables when scatter plots indicated a linear relation between the radionuclide or TC and clay content. For this study each subset (each field, region and district) was randomly divided into a calibration and a validation dataset. This method is referred to as data-splitting (Brus *et al*., 2011). It should be noted that the observation locations of the calibration and validation set are randomly chosen after stratification on TC readings to ensure wide ranges of radionuclide readings. Although absolutely random selection of the validation locations in the field might have been better, the random data-splitting approach does yield meaningful information (Brus *et al*., 2011). The calibration sets of all the districts were combined to analyse the three selected Dutch marine districts together.

Using the calibration sets, a linear regression model of the radionuclides or TC against clay content was created for the total

Table 1 Overview of the marine districts and the identified regions within the districts; soil series are as described by Steur & Heijink (1991)

	Region	
District	Geomorphology	Soil series
Southwestern marine district (SMD)	New-land polder	Calcareous hydromorphic marine soils (Mn..A)
IJsselmeerpolder district (IJPD)	Former lake bottoms	Calcareous hydromorphic marine soils (Mn..A)
Northern marine district (NMD)	Salt marsh basin	Calcareous hydromorphic marine soils (Mn..A)
		Non-calcareous hydromorphic marine soils (Mn..C)
		Non-calcareous hydromorphic marine soils with low Ca/Mg ratio (gMn..C)
	Salt marsh barrier	Calcareous hydromorphic marine soils (Mn..A)
		Non-calcareous hydromorphic marine soils (Mn..C)
		Non-calcareous hydromorphic marine soils with low Ca/Mg ratio (gMn..C)

marine area, each district, each region and for four fields in the SMD area. The appropriate calibration model was then used to predict clay contents in the validation set based on gamma-ray signals. The output from the linear regression model was compared with the results from the calibration set of mean clay contents and the mean-based model:

$$Clay\% = \beta_0. \quad (3)$$

The following parameters were used to assess the results. For the calibration, the R^2 value (multivariate r^2 corrected for multiple inputs) is given as an indication of the strength of the linear regression. We checked whether the range of clay contents predicted by the linear regression models was similar to that of measured values in the datasets. This was done by comparing the standard deviation (SD) of the validation prediction with the SD of the measured dataset. Mean values in the calibration and validation datasets were also compared. The absolute error was computed with the root mean squared error (RMSE) (Equation (4):

$$RMSE = \sqrt{\frac{\sum_{N=1}^{N} (Y_p - Y_m)^2}{N}}, \quad (4)$$

where Y_p is the predicted value, Y_m is the measured value and N is the number of measurements in the calibration or validation set.

Comparison of the RMSEs in the validation dataset of the mean-based model, using the calibration mean as predictor, with those of the linear regression predictor models shows whether linear regression using radionuclides improves prediction.

Results

Descriptive statistics

Table 2 shows descriptive statistics of the radionuclides for the different districts. The IJPD had a larger range and more variation in the radionuclides than the other districts. Visual inspection of the distribution of clay content among the districts (Figure 3) showed that these approach a normal distribution.

Table 2 Descriptive statistics for the radionuclides in the three marine districts: SMD (southwestern marine district), IJPD (IJsselmeerpolder district) and NMD (northern marine district)

Radionuclide		Mean	SD
^{40}K / Bq kg^{-1}	SMD	422	49
	IJPD	390	74
	NMD	430	44
^{232}Th / Bq kg^{-1}	SMD	27	5
	IJPD	26	7
	NMD	30	4
TC[a] / s^{-1}	SMD	175	27
	IJPD	166	39
	NMD	190	24

[a]TC = total count.

Field-scale models

Field-scale models were constructed for four fields in the SMD, each of approximately 0.4 km^2 and consisting of the *Mn..A* soil series within new-land polders. These fields were chosen because they had sufficient data for both calibration and validation. As a result of the small sample size, the calibration and validation sets have similar but not identical means and standard deviations (Table 3).

For all fields, application of the regression models to the validation dataset resulted in a smaller RMSE compared with the mean-based model (Table 3), although for field 2 the variation in the data was already small (Figure 4). The regression models provided good predictions of means and had variation similar to the datasets, even though the calibration and validation datasets had different means. The TC and radionuclides ^{40}K and ^{232}Th proved to be good explanatory variables with no clear preference in R^2 values. Fields 3 and 4 are adjacent and had similar results. The regression lines of ^{40}K for these fields show one unique fingerprint, whereas ^{232}Th and TC have three lines parallel to each other.

Regional scale models

The descriptive statistics of the calibration and validation sets for each region (Table 4) show that the areas with *Mn..A* soil series in relatively flat and low-lying areas have the largest variation in clay content. In the NMD, mean clay contents in salt marsh basins were always greater compared with mean clay contents in salt marsh barriers. When compared with the field-scale datasets, the calibration and validation sets have more similar distributions, because of the larger number of samples.

In the regions in the SMD and IJPD, application of the linear regression models with ^{40}K and ^{232}Th to the validation dataset resulted in smaller RMSEs as compared with that of the mean-based model (Table 4). The regression models had a mean and standard deviation for the predictions comparable to those of the calibration dataset. The regression predictions for TC were similar to those of the mean-based model in the validation dataset. Within the NMD, application of most regional regression models to the validation dataset resulted in RMSEs comparable to those of the mean-based models. For the *Mn..C* and *gMn..C* soil series in the NMD barriers and basins and for the *Mn..A* soil series within the barriers this is attributed to the small variation in clay contents in the datasets, which is comparable to the laboratory error. The *Mn..A* series in the salt marsh basins of the NMD had more variation and the RMSEs of the linear regression models are smaller compared with that of the mean-based model. The predicted mean and range were similar to the dataset. In this region the values for R^2 are relatively small compared with the results for the regions in the IJPD and SMD.

District scale models

At the district scale the SMD has the largest mean clay contents (Table 5). The NMD had less variation in clay content than the

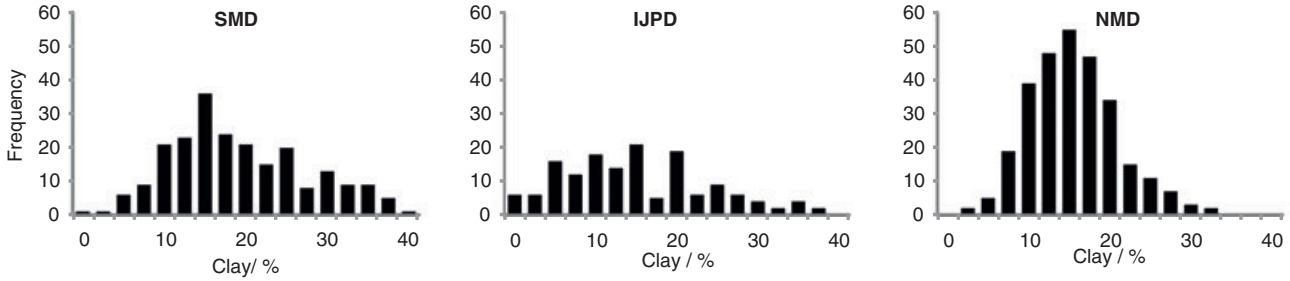

Figure 3 Distribution of clay content in the calibration datasets in the southwestern marine district (SMD), the IJsselmeerpolder district (IJPD) and the northern marine district (NMD).

Table 3 Statistics for the field-scale models using the calibration and validation datasets, indicating the root mean squared error (RMSE) and R^2 between models and measurements (calibration) and the RMSE between predictions and measurements (validation)

	Calibration				Validation (prediction)		
	Mean	SD	RMSE	R^2	Mean	SD	RMSE
Model	/ % clay				/ % clay		
Field 1 (nine calibration and nine validation samples) 0.44 km^2							
Mean-based[a]	27	7	7		25	10	9
^{40}K	26	6	4	0.65	25	6	2
^{232}Th	26	7	3	0.80	26	7	3
^{40}K&^{232}Th	26	7	3	0.78	25	7	3
TC[b]	27	6	3	0.72	26	10	2
Field 2 (eight calibration and eight validation samples) 0.42 km^2							
Mean-based[a]	18	2	2		19	4	4
^{40}K	18	1	2	0.23	19	1	3
TC[b]	18	1	1	0.17	18	1	3
Field 3 (eight calibration and seven validation samples) 0.39 km^2							
Mean-based[a]	25	5	5		29	7	8
^{40}K	25	5	2	0.85	29	5	4
^{232}Th	25	5	2	0.87	29	5	4
^{40}K&^{232}Th	25	5	1	0.95	29	5	4
TC[b]	25	5	1	0.93	29	4	3
Field 4 (seven calibration and six validation samples) 0.39 km^2							
Mean-based[a]	24	8	8		32	7	10
^{40}K	23	7	2	0.89	31	7	3
^{232}Th	24	7	2	0.91	34	7	3
^{40}K&^{232}Th	24	7	2	0.89	33	7	3
TC[b]	24	7	1	0.94	33	9	4

[a]The mean and standard deviations of the mean-based model are the mean and standard deviation of the calibration and validation sets.
[b]TC = total count.

other two districts. Following the calibration graphs for ^{40}K, ^{232}Th and TC (Figure 5), the SMD and IJPD provide linear regression models that have relatively large R^2 values (Table 5). The radionuclide ^{232}Th seems to be the best predictor on a district scale when based on R^2 and the computed RMSE in the validation dataset. The TC was not linearly related to clay content in the NMD (Figure 5) and was not taken into account in the validation analyses. For the SMD and IJPD, application of the TC regression models to the validation dataset resulted in larger RMSE values compared with regression models that included ^{232}Th.

Models for all the marine districts together

The calibration sets from all three districts were combined to test whether linear regression models could identify a unique fingerprint for sediments in these marine districts. From the scatterplots (Figure 6) and the given values for R^2 (Table 6) it can be concluded that TC again performs relatively poorly compared with ^{232}Th and ^{40}K. When compared with those for the SMD and IJPD, the national scale regression models have smaller R^2 values.

None of the regression models appeared to be capable of predicting clay content for all three districts together. Application of the linear regression models to the validation dataset resulted in RMSE values that are comparable to the RMSE of the mean-based model (Table 6). Linear regression using radionuclides therefore adds little value when compared with the model based on the mean. The regression models have slightly smaller ranges in their predictive outputs compared with the range in the dataset.

Because the regression lines of the SMD and IJPD show similarities in Figure 5, a combined analysis of these two districts was carried out. A regression model for these districts together (Table 7) had a similar performance compared with those for the individual districts (Table 5). This is a strong indication that these two districts have similar fingerprints.

Discussion

Comparison with other studies

At the field scale, the RMSE of the predictions for fields 1, 2 and 4 was reduced to 2–3% by using linear regression models compared with 8–10% for the mean-based model. Viscarra Rossel *et al.* (2007) found an average model RMSE of 6% compared with 11% for the mean-based model. The size of the fields in the Viscarra Rossel *et al.* (2007) study (about 2 km^2) was closer to the regional scales in our study where reductions of 8–6% were found. Most other studies have used airborne sensors with much coarser spatial resolutions, which makes comparison difficult.

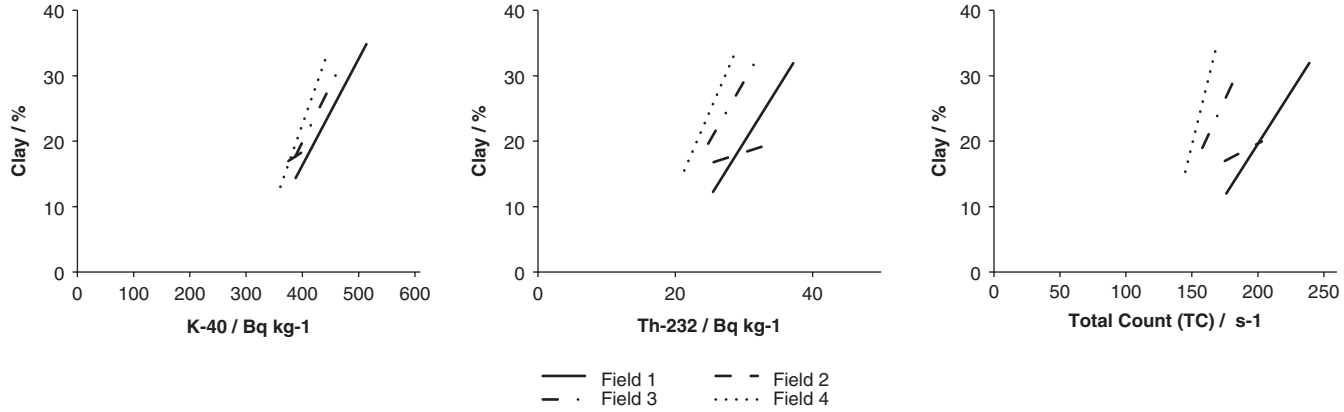

Figure 4 Linear regression models at the field scale (length of the lines gives range of radionuclides). Note the differences in scales on the horizontal axes.

Comparison of field, regional and district scale models for clay content

The smallest RMSE of the predictions for clay content at the field scale in the SMD was 2–3% (Table 3). On a regional scale in the SMD, the smallest RMSE value of the predictions was 5% (Table 4) whereas at the district scale the calculated RMSE of the predictions was 4% (Table 5). The errors at the regional and district scales are close to the measurement error with the laboratory method with the least accuracy. This suggests that the best performing models in the SMD for clay content are obtained through calibration at the field scale. However, if the number of soil samples limits calibration, linear regression models at a regional or district level can be used, as this approach still results in a decrease in RMSE from 9% with the mean-based model, to 4% with a linear regression model.

When the three total Dutch marine districts were taken together, the RMSE of 6% for the regression models, except for TC, is comparable to the RMSE of 7% when using the mean-based model. The performance of linear regression models at the largest scale investigated can therefore be considered as being poor.

Error propagation

Before spatial predictions are carried out, uncertainty and error can be propagated at any stage in the preprocessing operations. These are (i) acquisition of gamma-ray data and soil samples, (ii) soil sample laboratory analyses, (iii) extraction of activities of the radionuclides from the gamma-ray spectra and (iv) calibrating relationships between the radionuclides and the soil properties and their validation.

The soil samples used in the present study were collected at farmers' requests to describe the field-scale variability. This means that samples are not uniformly distributed for gamma-ray spectroscopy amongst the districts and regions. All samples were taken from arable fields. This influences the variation in input data, because, for example, fields with very large clay contents may be dominantly used for grassland because of difficulties in tillage operations.

In the second step, soil properties are measured in the laboratory. The laboratory reproducibility for clay content with the NIRS method was in some cases comparable to that within a dataset. The radionuclide concentrations were derived from the total spectrum using the FSA method, which had the least uncertainty according to published literature.

The third step, which is the focus of this study, can be further subdivided into (iiia) choosing the landscape factors to stratify the study area and (iiib) calibration and validation. The aim of stratification is to select areas with comparable relationships between the gamma-ray signal and a particular soil property. Determining factors may be, for example, parent material, topography and age. For regional stratification within districts, soil maps and geomorphological maps were used. At the borders of the mapping units the uncertainty is relatively large because most geomorphological boundaries in the marine districts are gradual. Samples in the gradual transition areas may have been misclassified.

Salt marsh barriers were one of the geomorphic mapping units used to stratify the northern marine district. However, the barriers differ in width, altitude, size, deposition age and current distance from the coast. The same variation is applicable to the salt marsh basins. In our case, samples from different fields were combined in the regional-scale models for uniform geomorphic units but a further subdivision with respect to, for example, age may result in models with smaller RMSE values. Further, a catena might be present in the salt marshes in the polders, where top-soil clay content often decreases from the older to younger dykes.

In step (iiib) the relationships are calibrated. This is done with a specified set of radionuclides and soil properties for which the linearity was investigated. A normal distribution of the data is not guaranteed in the case of small datasets, such as was the case for the field-scale data.

Table 4 Statistics for the regional-scale models using the calibration and validation datasets, indicating the root mean squared error (RMSE) and R^2 between models and measurements (calibration) and the RMSE between predictions and measurements (validation)

	Calibration				Validation (prediction)		
	Mean	SD	RMSE	R^2	Mean	SD	RMSE
Model	/ % clay				/ % clay		
SMD – plains - Mn..A region (188 calibration and 179 validation samples)							
Mean-based[a]	21	8	8		21	8	8
^{40}K	21	5	5	0.48	21	6	6
^{232}Th	21	6	4	0.67	21	6	5
^{40}K&^{232}Th	21	6	4	0.67	21	6	5
TC[b]	21	5	6	0.45	20	4	8
IJPD – former lake bottom - Mn..A region (88 calibration and 102 validation samples)							
Mean-based[a]	18	7	7		19	9	9
^{40}K	17	5	5	0.56	18	5	7
^{232}Th	17	5	5	0.59	18	5	6
^{40}K&^{232}Th	18	5	4	0.59	18	5	6
TC[b]	17	5	5	0.45	19	5	11
NMD – salt marsh basin - Mn..A region (53 calibration and 52 validation samples)							
Mean-based[a]	21	7	7		21	7	7
^{40}K	21	4	6	0.31	21	4	4
^{232}Th	21	5	5	0.40	20	5	4
^{40}K&^{232}Th	21	5	5	0.40	21	5	4
TC[b]	21	4	6	0.26	21	4	5
NMD – salt marsh basin - Mn..C region (14 calibration and 24 validation samples)							
Mean-based[a]	19	4	4		17	4	4
^{40}K	19	4	2	0.68	19	4	3
^{232}Th	19	4	2	0.65	20	4	4
^{40}K&^{232}Th	19	4	2	0.66	20	4	4
NMD – salt marsh basin - gMn..C region (24 calibration and 40 validation samples)							
Mean-based[a]	17	4	4		19	3	4
^{40}K	17	2	3	0.34	18	2	3
^{232}Th	17	3	2	0.77	18	3	3
^{40}K&^{232}Th	17	3	2	0.76	18	3	3
TC[b]	17	3	2	0.53	18	3	4
NMD – salt marsh barrier - Mn..A region (106 calibration and 115 validation samples)							
Mean-based[a]	15	4	4		16	6	6
^{40}K	15	2	4	0.29	15	2	5
^{232}Th	15	3	4	0.33	15	3	4
^{40}K&^{232}Th	15	4	4	0.34	16	6	6
TC[b]	15	2	4	0.12	15	2	5
NMD – salt marsh barrier - Mn..C region (38 calibration and 48 validation samples)							
Mean-based[a]	15	4	4		15	5	5
^{40}K	15	2	4	0.25	14	2	5
^{232}Th	15	3	3	0.60	14	3	5
^{40}K&^{232}Th	15	3	3	0.60	14	3	5
NMD – salt marsh barrier - gMn..C region (20 calibration and 26 validation samples)							
Mean-based[a]	16	3	3		16	4	4
^{40}K	16	3	3	0.63	16	3	3
^{232}Th	16	2	2	0.18	17	2	3
^{40}K&^{232}Th	16	3	2	0.61	16	2	3

[a]The mean and standard deviations of the mean-based model are the mean and standard deviation of the calibration and validation sets.
[b]TC = total count. SMD, southwestern marine district; IJPD, IJsselmeer-polder district; NMD, northern marine district.

Table 5 Statistics for the district scale models using the calibration and validation datasets, indicating the root mean squared error (RMSE) and R^2 between models and measurements (calibration) and the RMSE between predictions and measurements (validation)

	Calibration				Validation (prediction)		
	Mean	SD	RMSE	R^2	Mean	SD	RMSE
Model	/ % clay				/ % clay		
SMD (222 calibration and 241 validation samples)							
Mean-based[a]	20	8	8		21	8	8
^{40}K	20	6	5	0.57	20	6	6
^{232}Th	20	7	5	0.70	21	7	4
^{40}K&^{232}Th	20	7	5	0.70	21	7	4
TC[b]	20	6	6	0.50	21	6	6
IJPD (150 calibration and 176 validation samples)							
Mean-based[a]	16	9	9		16	9	9
^{40}K	16	6	6	0.51	15	6	6
^{232}Th	16	7	5	0.65	15	7	6
^{40}K&^{232}Th	16	7	5	0.65	15	7	6
TC[b]	16	6	6	0.53	15	6	7
NMD (287 calibration and 295 validation samples)							
Mean-based[a]	17	5	5		17	6	6
^{40}K	17	3	4	0.35	16	3	5
^{232}Th	16	4	4	0.43	17	4	4
^{40}K&^{232}Th	17	4	4	0.44	17	4	4

[a]The mean and standard deviations of the mean-based model are the mean and standard deviation of the calibration and validation sets.
[b]TC = total count. SMD, southwestern marine district; IJPD, IJsselmeer-polder district; NMD, northern marine district.

Effect of differences in clay mineralogy

The models with the smallest RMSE were those that used ^{40}K and/or ^{232}Th or TC. Within soils, ^{40}K content is related to secondary minerals such as illite, whereas ^{238}U and ^{232}Th contents are related to Fe- and Ti-oxides (Cattle *et al*., 2003). The clay deposited in the SMD originates from the southern rivers such as the Meuse and the Rhine. The IJsselmeerpolders also received primarily material from the Rhine. The northern marine district has received a mixture of marine material from the Elbe river (De Meijer & Donoghue, 1995) but also sediments from the Rhine and Meuse, because currents along the Dutch coast transport sediments from south to north. We speculate that this causes marine deposits in the IJPD and SMD to be more homogeneous in clay mineralogy and thus have one typical fingerprint, where the NMD might contain several. Apparently the influence of northern Wadden Sea sediments is limited in IJPD. As shown in Table 7 for the SMD and IJPD together, application of the models based on ^{232}Th or ^{40}K&^{232}Th to the validation dataset results in RMSE values that are smaller compared with that of the mean-based model. Therefore the relationship between gamma-ray signals and soil properties might be less clear in the NMD. Unfortunately, little is known about the clay mineralogy of the marine districts of the Netherlands. Differences in clay mineralogy have been reported

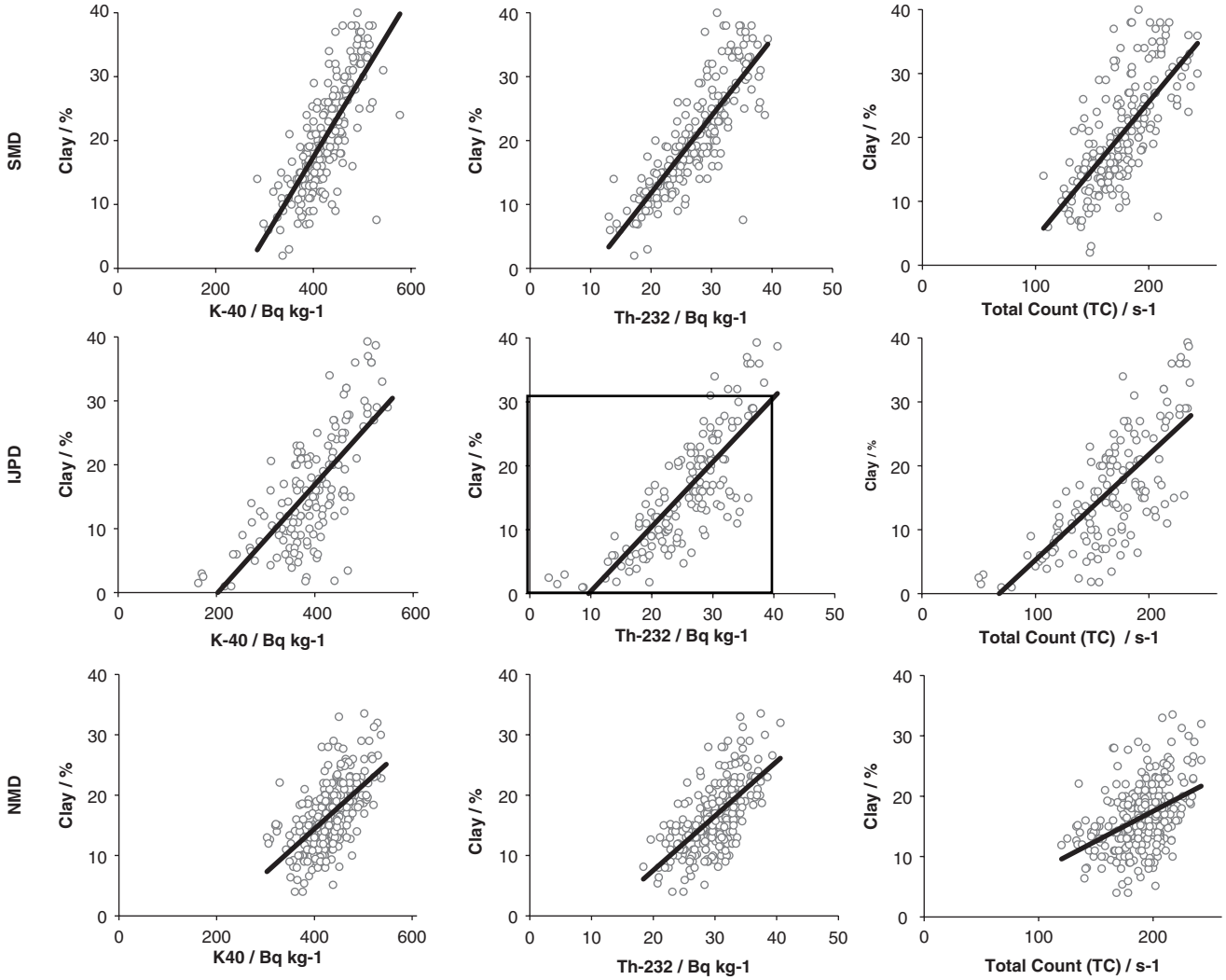

Figure 5 Scatter plots of clay content and radionuclides (^{40}K, ^{232}Th and TC) at the district scale using the calibration datasets. Note the differences in scales on the horizontal axes.

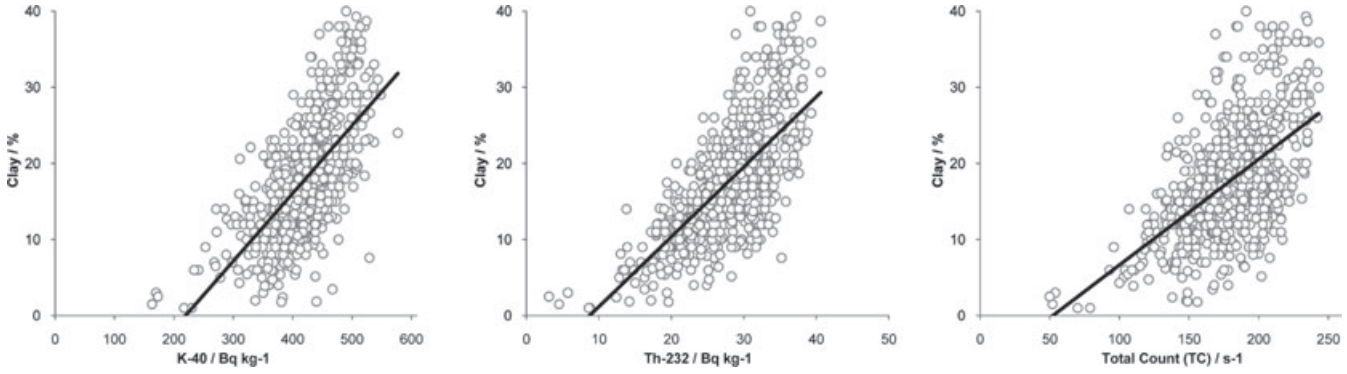

Figure 6 Scatter plots of clay content and radionuclides (^{40}K, ^{232}Th and TC) for all the Dutch marine clay districts together. Note the differences in scales on the horizontal axes.

Table 6 Statistics for the models for all marine districts together using the calibration and validation datasets, indicating the root mean squared error (RMSE) and R^2 between models and measurements (calibration) and the RMSE between predictions and measurements (validation)

	Calibration				Validation (prediction)		
	Mean	SD	RMSE	R^2	Mean	SD	RMSE
Model	/ % clay				/ % clay		
SMD + IJPD + NMD (659 calibration and 712 validation samples)							
Mean-based[a]	18	8	8		18	7	7
^{40}K	18	5	6	0.44	17	5	6
^{232}Th	18	5	5	0.48	18	5	6
^{40}K&^{232}Th	18	5	6	0.50	18	6	6
TC[b]	18	4	6	0.32	17	4	6

[a]The mean and standard deviations of the mean-based model are the mean and standard deviation of the calibration and validation sets.
[b]TC = total count. SMD, southwestern marine district; IJPD, IJsselmeerpolder district; NMD, northern marine district.

Table 7 Statistics for the models of the combined southwestern district (SMD) and IJsselmeerpolder district (IJPD) using the calibration and validation datasets, indicating the root mean squared error (RMSE) and R^2 between models and measurements (calibration) and the RMSE between predictions and measurements (validation)

	Calibration				Validation (prediction)		
	Mean	SD	RMSE	R^2	Mean	SD	RMSE
Model	/ % clay				/ % clay		
SMD + IJPD (372 calibration and 417 validation samples)							
Mean-based[a]	19	9	9		19	8	8
^{40}K	19	6	6	0.55	18	7	6
^{232}Th	19	7	5	0.67	18	7	5
^{40}K&^{232}Th	19	7	5	0.67	18	6	5
TC[b]	19	6	6	0.51	18	7	6

[a]The mean and standard deviations of the mean-based model are the mean and standard deviation of the calibration and validation sets.
[b]TC = total count.

between fluvial and marine sediments (Breeuwsma, 1985), but not between marine sediments from different districts.

Conclusions

Gamma-ray spectrometry is a high-resolution, cost-effective method for predicting clay contents at the field scale. At field scales, application of linear regression models based on ^{40}K, ^{232}Th, ^{40}K&^{232}Th or TC to validation datasets had RMSE values of 3–4%; this compared with a RMSE of 8–10% with a model based on the mean. For regions with comparable geomorphology and soil series, application of linear regression models in the southwestern marine district and the IJsselmeerpolder district gave RMSE values around 6% compared with 9% when using the mean of the dataset as a predictor, especially when ^{232}Th was included. TC alone was not a reliable predictor at this scale. In regions in the northern marine district, linear regression models did not result in smaller RMSE values compared with the mean of the datasets, possibly because of the smaller ranges of variation. The lower-lying calcareous soils are exceptions to this because these had a similar linear regression prediction capability to that for regions in the IJsselmeerpolder and the southwestern districts. At the district scale, smaller RSME values were found for linear relationships between clay content and radionuclides, again especially when ^{232}Th was included. For the southwestern marine and the IJsselmeerpolder districts, values for R^2 varied between 0.50 and 0.70. Values for R^2 were much smaller for the northern marine district, most probably because of the multiple origins of sediments with different fingerprints. No unique fingerprint existed between clay content and gamma-ray signal for all the Dutch marine districts taken together, and the RMSE of 6% is not much different from that of 7% when using the overall mean as a predictor.

Because relationships between gamma-ray signals and clay contents will probably be more robust for areas with comparable lithologies, such as the southwestern and IJsselmeerpolder districts, the prediction of clay contents using gamma-ray spectrometry is feasible in young Holocene deltaic environments, provided that the origin of the sediments results in a unique fingerprint.

Acknowledgements

We would like to thank Gerard Heuvelink for his advice on statistical matters. We would also like to thank Ronald Koomans for his input on fingerprinting. Furthermore, we would like to thank Heko Köster for his comments on an earlier version of this paper.

References

Breeuwsma, A. 1985. *Kleimineralogische en chemische karakteristieken van zeeklei, rivierklei en beekklei (Clay mineralogical and chemical characteristics of marine clay, river clay and brook clay)*. Stichting voor Bodemkartering, Wageningen.

Brus, D.J., Kempen, B. & Heuvelink, G.B.M. 2011. Sampling for validation of digital soil maps. *European Journal of Soil Science*, **62**, 394–407.

Cattle, S.R., Meakin, S.N., Ruszkowski, P. & Cameron, R.G. 2003. Using radiometric data to identify aeolian dust additions to topsoil of the Hillston district, western NSW. *Australian Journal of Soil Research*, **41**, 1439–1456.

Cook, S.E., Corner, R.J., Groves, P.R. & Grealish, G.J. 1996. Use of airborne gamma radiometric data for soil mapping. *Australian Journal of Soil Research*, **34**, 183–194.

De Bakker, H. 1979. *Major Soils and Soil Regions in the Netherlands*. Junk B.V. & Pudoc, Wageningen.

De Groot, A.V., Van der Graaf, E.R., De Meijer, R.J. & Maučec, M. 2009. Sensitivity of in-situ γ-ray spectra to soil density and water content. *Nuclear Instruments & Methods in Physics Research A*, **600**, 519–523.

De Meijer, R.J. & Donoghue, J.F. 1995. Radiometric fingerprinting of sediments on the Dutch, German and Danish coasts. *Quaternary International*, **26**, 43–47.

De Vries, F., De Groot, W.J.M., Hoogland, T. & Denneboom, J. 2003. *De Bodemkaart van Nederland Digitaal (The Digital Soil Map of the Netherlands).* Alterra, Wageningen.

Frissel, M.J., Stoutendijk, J.F., Koolwijk, A.C. & Köster, H.W. 1987. The Cs-137 contamination of soils in the Netherlands and its consequences for the contamination of crop products. *Netherlands Journal of Agricultural Science*, **35**, 339–346.

Hebinck, K., Middelkoop, H., Van Diepen, N., Van Der Graaf, E.R. & De Meijer, R.J. 2007. Radiometric fingerprinting of fluvial sediments in the Rhine-Meuse delta, the Netherlands – a feasibility test. *Geologie en Mijnbouw/Netherlands Journal of Geosciences*, **86**, 229–240.

Hendriks, P.H.G.M. 2002. *Simulatie van standaardspectra ten behoeve van veldmetingen (Simulation of Standard Spectra forField Measurements).* Medusa, Groningen.

Hendriks, P.H.G.M., Limburg, J. & De Meijer, R.J. 2001. Full-spectrum analysis of natural γ-ray spectra. *Journal of Environmental Radioactivity*, **53**, 365–380.

IUSS 2006. *World Reference Base for Soil Resources 2006*. World Soil Resources Reports No 103, FAO, Rome.

Kemmers, R.H., Van Egmond, F.M. & Loonstra, E.H. 2008. *Kartering van fosfaatbeschikbaarheid in de bodem met behulp van natuurlijke radioactiviteit (Mapping Phosphate Availability in the Soil using Natural Radioactivity).* Alterra, Wageningen.

Koomen, A.J.M. & Maas, G.J. 2004. *Geomorfologische kaart Nederland; achtergrond bij het landsdekkende digitale bestand (Geomorphological Map of the Netherlands; Background to the Full-Cover Digital Dataset).* Alterra, Wageningen.

Köster, H.W., Mattem, F.C.M. & Pennders, R.M.J. 1987. *The Radioactive Contamination of the Soils in the Netherlands due to the Nuclear Accident at Chernobyl.* Working documents volume 2, CCRX. Ministry of Housing and Environment (VROM), Leidschendam.

Köster, H.W., Keen, A., Pennders, R.M.J., Bannink, J.H. & De Winkel, J.H. 1988. Linear regression models for the natural radioactivity (U-238, Th232 and K-40) in Dutch soils: a key to anomolies. *Radiation Protection Dosimetry*, **24**, 63–68.

Pracilio, G., Adams, M.L., Smettem, K.R.J. & Harper, R.J. 2006. Determination of spatial distribution patterns of clay and plant available potassium contents in surface soils at the farm scale using high resolution gamma ray spectrometry. *Plant & Soil*, **282**, 67–82.

Rawlins, B.G., Lark, R.M. & Webster, R. 2007. Understanding airborne radiometric survey signals across part of eastern England. *Earth Surface Processes & Landforms*, **32**, 1503–1515.

Söderström, M. & Eriksson, J.E. 2008. Gamma-ray sensing for cadmium risk assessment in agricultural soil and grain – a case study in eastern Sweden. In *1st Global Workshop on High Resolution Digital Soil Sensing and Mapping*, *Sydney*. Workshop Program and Papers Volume II, 8p, University of Sydney 2008, Sydney.

Statistics Netherlands 1993. *Landbouwgebiedsindeling 1991 (Agricultural Regions 1991).* Statistics Netherlands, Voorburg/Heerlen.

Steur, G.G.L. & Heijink, W. 1991. *Bodemkaart van Nederland, schaal 1:50,000; algemene begrippen en indelingen (Soil Map of the Netherlands, Scale 1:50 000; General Concepts and Categories).* Staring Centrum, Wageningen.

Stiboka 1981. *Bodemkaart van Nederland schaal 1:50 000, kaartbladen 2 en 6 (Soil Map of the Netherlands Scale 1:50 000, Map sheets 2 and 6).* Stichting voor Bodemkartering, Wageningen.

Van Alphen, B.J. & Stoorvogel, J.J. 2000. A functional approach to soil characterization in support of precision agriculture. *Soil Science Society of America Journal*, **64**, 1706–1713.

Van Egmond, F.M., Loonstra, E.H. & Limburg, J. 2010. Gamma ray sensor for topsoil mapping; the mole. In: *Proximal Soil Sensing* (eds R.A. Viscarra Rossel, A. McBratney & B. Minasny), pp. 323–332. Springer, Dordrecht.

Van Wijngaarden, M., Venema, L.B., De Meijer, R.J., Zwolsman, J.J.G., Van Os, B. & Gieske, J.M.J. 2002. Radiometric sand/mud characterisation in the Rhine-Meuse estuary; part A. Fingerprinting. *Geomorphology*, **43**, 103–116.

Viscarra Rossel, R.A. & McBratney, A.B. 1998. Laboratory evaluation of a proximal sensing technique for simultaneous measurement of soil clay and water content. *Geoderma*, **85**, 19–39.

Viscarra Rossel, R.A., Taylor, H.J. & McBratney, A.B. 2007. Multivariate calibration of hyperspectral γ-ray energy spectra for proximal soil sensing. *European Journal of Soil Science*, **58**, 343–353.

Wong, M.T.F. & Harper, R.J. 1999. Use of on-ground gamma-ray spectrometry to measure plant-available potassium and other topsoil attributes. *Australian Journal of Soil Research*, **37**, 267–277.